Journal Name

COMMUNICATION

Ultrathin Niobate Nanosheet Nanofiltration Membranes for Water Treatment

Received 00th January 20xx,
Accepted 00th January 20xx

DOI: 10.1039/x0xx00000x

www.rsc.org/

K. Nakagawa,*[a] H. Yamashita,[b,c] D. Saeki,[c] T. Yoshioka,[a] T. Shintani,[a] M. Katoh,[b] S. Sugiyama,[b] S. C. E. Tsang,[d] E. Kamio,[c] and H. Matsuyama[c]

Two dimensional niobate nanosheets are assembled into ultrathin membrane by a simple vacuum filtration. The nanosheet nanofiltration membranes have a dense and stable structure in water and show high rejection performance (nealy 100% of Evanz bule and 78.4% for Na_2SO_4). A short water pathway model based on a void structure formation is presented for explaining the fast water diffusion.

Water treatment techniques using membrane-based separation have great advantages such as lower energy consumption, less space, higher separation selectivity and continuous operation as compared with other traditional waste water treatment. Inorganic membranes have excellent thermal, mechanical and structural strength and chemical resistance, therefore, many application in water treatment have been studied. Well-defined inorganic nanostructures, such as silica-based materials, zeolites, metal organic frameworks and carbon-based materials have attracted much attention in membrane separation application for desalination and pervaporation. An ideal separation membrane for water treatment is expected to have a separation layer as thin as possible to maximize a permeation flux and have appropriate pore sizes to obtain an excellent rejection ratio.[1] In order to achieve the goal, new types of inorganic membranes with advanced structure should be designed.

Recently, two-dimensional (2D) nanosheet membranes has opened up a new avenue for fabricating size-selective molecular separation membranes due to their unique atomic thickness with micrometer lateral dimensions, high mechanical strength and chemical inertness. Nanosheet membranes can be formed by assembling nanosheets into stacked thin membrane and 2D nanochannels between the stacked sheets allow water to pass through while rejecting unwanted solutes. So far, graphene oxide[2–11] and transition metal dichalcogenides[12,13] have been studied for stacked nanosheet membranes. Especially many efforts have been made to fabricate GO-based membranes with high flux and separation performances by taking advantage of the interlayer nanochannels between GO sheets. However, only a few different types of nanosheet were mainly focused although many kinds of nanosheet materials have been reported. Transition metal oxide nanosheets[14,15] offer attractive surface and catalytic properties[16–20] and can be assembled into stacked thin membrane. Therefore, transition metal oxide nanosheets become promising materials for potentially high functional membrane for water separation. Very recently, hybrid membranes consisting of GO nanosheets and titania nanosheets[21] or Co-Al (or Mg-Al) layered double hydroxide nanosheets[22] have been reported for the application of desalination or waste water treatment. Nanosheet membranes consisting of only transition metal oxide is however not yet demonstrated. Structural stability of nanosheet membranes in water is another critical issue for their application because such 2D nanosheets become negatively charged on hydration and the membrane should disintegrate owing to electrostatic repulsion, which results in the redispersion of these nanosheets.[23] Such membranes were unable to survive the cross-flow testing condition which is typical in membrane operation. In fact, a dead-end filtration was often utilized for the separation performance of nanosheet membranes. Stable bonding between nanosheets and that between nanosheets and support should be a key issue to prevent their dispersion in water.

Here, we firstly report a novel nanosheet (NS) membranes using single 2D molecular sheets of niobate. Niobate nanosheets prepared by a bottom-up approach using hydrothermal synthesis in the presence of triethanolamine (TEOA) were assembled on a surface-modified cellulose nitrate

[a] *Center for Membrane and Film Technology, Graduate School of Science, Technology and Innovation, Kobe University, Kobe 657-8501, Japan. E-mail: knakagaw@port.kobe-u.ac.jp*
[b] *Department of Science and Technology, Faculty of Science and Technology, Tokushima University, Tokushima 770-8506, Japan.*
[c] *Center for Membrane and Film Technology, Department of Chemical Science and Engineering, Kobe University, Kobe 657-8501, Japan.*
[d] *Department of Chemistry, University of Oxford, Oxford, OX1 3QR, UK.*
† Electronic Supplementary Information (ESI) available. See DOI: 10.1039/x0xx00000x

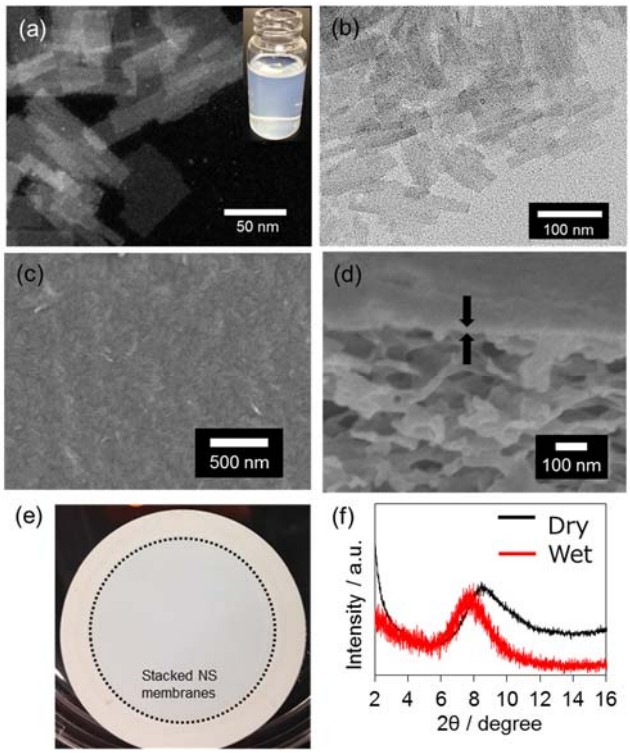

Figure 1. (a) STEM and (b) TEM images of niobate molecular sheets, inset: A picture of NS colloidal suspension; (c) Overview and (d) cross-section FE-SEM image of NS membrane; (e) Pictures of NS membranes after shaking the membrane immersed in water in a petri dish for three days; (f) XRD patterns of NS membranes (with a thickness of 90 nm). Black line: dry condition, Red line: wet condition.

(CN) support by a simple vacuum filtration. It is found that the stacked niobate NS membranes have a dense structure and are highly stable during separation tests using a cross-flow membrane filtration system, because TEOA molecules act as a chemical binder between nanosheets. The simple method also allows creation of nanochannels in the stacked NS membrane, which is found to be high-flux nanofiltration membranes with superior rejection performances of salts.

Single molecular layers of niobate were prepared by a bottom-up approach[20] using hydrothermal method of niobium(V) ethoxide ($Nb(OEt)_5$) as niobium source in ammonium aqueous solution in the presence of TEOA (see ESI). Then, niobate nanosheets are assembled on a CN support by a vacuum filtration. Structural analyses of the prepared samples and membranes were carried out by STEM, TEM, FE-SEM and XRD (**Figure 1**). A colloidal solution was obtained by hydrothermal method and distinct flat single molecular layer sheets with sharp edges were observed in the prepared sample (**Figures 1**(a) and (b)). In the hydrothermal synthesis, the chemical reactions of $Nb(OEt)_5$ and water occur to create nucleation and growth of niobium oxide. In order to control the evolution of the niobium oxide structure in 2-D and morphology, TEOA was used as a adsorbing-chelating ligand for $Nb(OEt)_5$ which plays a key role to stabilize of Nb against rapid hydrolysis in alkaline solution. As a result, the single molecular layer sheets can be stabilized against stacking.[20] **Figures 1**(c) and (d) show surface and cross-section SEM images of NS membranes. Smooth surface is observed on the NS membranes while many pores with 10 - 100 nm in diameter are observed in CN support and the CN support modified with 3-aminopropyl-triethoxysilane (APTES) (CN-APTES) (ESI), which indicate the whole surface of the CN support is entirely coated with niobate nanosheets in the NS membrane. It is noted that niobate nanosheets were partially peeled off from CN support after shaking the membrane immersed in water in a petri dish for three days, whereas the nanosheets deposited stably on the CN-APTES support (**Figure 1**(e) and Figure S5 in ESI). Hereafter CN-APTES support was used for NS membranes. The cross-section image (**Figure 1**(d)) shows that thickness of the NS membrane is about 20 nm. The each niobate nanosheets seem to be connected each other and form flat ultrathin layer on CN-APTES support during the vacuum filtration. The thickness of NS membranes can be controlled from 20 – 90 nm by changing a volume of NS colloidal solution for the vacuum filtration (ESI). **Figure 1**(f) highlights XRD patterns of NS membranes with a thickness of 90 nm. In dry conditions, the broad peak at 8.6°, corresponding to (020) diffraction of stacked nanosheets with an interlayer spacing of 1.0 ± 0.05 nm, can be clearly seen in the NS membrane.

The stability tests of NS membranes were performed by shaking the membrane immersed in water in a petri dish for three days. For comparison, stacked graphene oxide (GO) membranes were also prepared in a similar vacuum filtration using GO colloidal solution synthesized by an improved Hummers' method[24] on the CN-APTES support (GO/CN-APTES). GO nanosheets were apparently peeled off from CN-APTES support after shaking in water, whereas the niobate nanosheets were stable on the CN-APTES support (Figure S7 in ESI). Furthermore, upon inspecting the structural changes in water by XRD patterns, slight increase of the interlayer distance from 1.0 to 1.1 nm was observed for NS membranes (**Figure 1**(f)), whereas a drastic increase of the interlayer distance from 0.7 to 1.5 nm was observed for GO membranes (ESI). These results clearly indicate that NS membranes have a highly stable structure in water. Considering that the thickness of the single niobate sheet is 0.9 nm,[20] a clearance gap between sheet layers is turned out to be only 0.2 nm.

It is thus interesting to find that this vacuum filtration approach using niobate nanosheet colloidal solution can give a highly stable structure in water for the NS membranes. In our membrane preparation method, the potential for this structural stability in water arises from two factors: one is an interaction between nanosheets and CN-APTES support, and another is that between nanosheet layers. It is found that surface modification of CN support using APTES prevents a redispersion of nanosheets from support. APTES molecules are often used as a chemical binder between a support and an active layer.[25,26] It is assumed that ethoxy groups of the APTES react with hydroxyl groups of cellulose compound included in CN support at the pretreatment of support with APTES, and amino groups react with the hydroxyl groups of niobate nanosheets via electrostatic

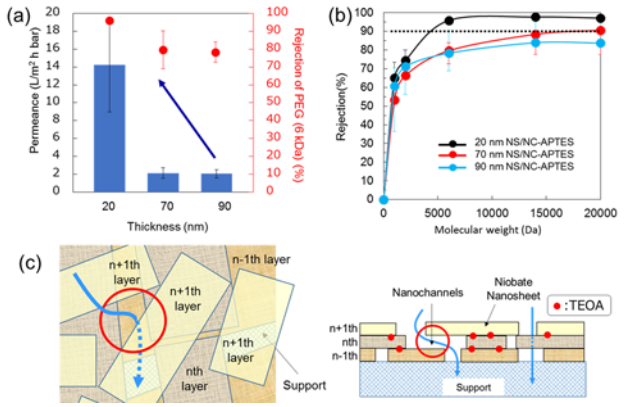

Figure 2. (a) Permeance (left axis) and rejection of PEG (Mw: 6kDa) (right axis) of NS membranes with different thickness; (b) MWCO indicated with the dashed line at 90% rejection of NS membranes with different thickness, evaluated with PEG of various MWs ranging from 1 to 20 kDa; (c) Schematic diagram of nanochannels in NS membranes seen from top view (left) and cross section (right).

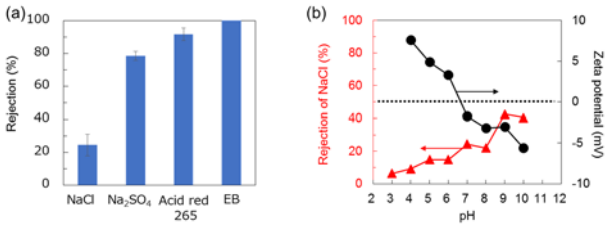

Figure 3. (a) Rejection performances of the NS membranes with a thickness of 20 nm for each salt; (b) Rejection of NaCl (left axis) and zeta potential (right axis) as function of pH for NS membranes with a thickness of 20 nm.

interaction during the vacuum filtration and drying processes, resulting in the enhancement of an interaction between niobate nanosheets and CN-APTES support. Next, the interaction between nanosheet layers are considered. In a colloidal aqueous solution including nanosheets and ammonia, negatively charged molecular sheets were stabilized against stacking in the presence of TEOA as strong surface adsorbate molecules.[20] During a vacuum filtrtration using the nanosheet colloidal sotluion, these nanosheets restack to form a ultrathin layer on CN-APTES support. When the vacuum drying time increases, the interlayer distance of NS membranes gradually decreases with time (ESI). These results indicate the removal of hydrated waters in the stacked sheets and NS membranes become so tightly packed. Furthermore, for XPS analysis, N1s peak was detected in the stacked NS membranes on polycarbonate support (ESI), implying the existance of TEOA in the prepraed membrane. We assume that TEOA react with the niobate nanosheets via electrostatic interaction and/or hydrogen bonding. Thus, TEOA molecules can effectively crosslink the sheet layers and strengthen the final membrane after vaccum drying, as is reported with organic molecules or divalent metal ions.[5,23] We believe that the facilitated formation of highly stable membranes in water using 2-D niobate molecular layers is important which would shed light on rational design, assembly and more effective applications of separation membranes using metal oxide nanosheets.

As a result, membrane performances of NS membranes were evaluated using a cross-flow membrane filtration system. **Figure 2**(a) shows the permeance and rejection ratio of polyethylene glycol (PEG, Mw: 6kDa) for NS membranes with different thickness. Thinner the thickness of NS membrane, higher permeance were obtained. High rejection ratio over 80% were obtained for all NS membranes, especially NS membranes with a thickness of 20 nm showed highest rejection ratio of 96 %, while CN support or CN-APTES support without NS layers showed extremely low rejection ratio less than around 10 % for PEG (20 kDa) (ESI). Molecular weight cutoff (MWCO) of the NS membranes was analyzed to use polyethylene glycol (PEG) with different molecular weights (**Figure 2**(b)). The results indicated MWCO decrease with decreasing the thickness of NS membranes. Values of 90 % MWCO were 4.3 and 17.0 kDa for NS membranes with a thickness of 20 and 70 nm, respectively. From the Stokes-Einstein radius which was determined by viscosimetry,[27] these values of molecular weight can be estimated as 1.7 nm for 4.3 kDa and 3.4 nm for 17.0 kDa. Thus, in view of MWCO measurements using PEG, it was found that the nanochannels with a diameter of 3.4 and 6.8 nm were formed in the NS membranes with a thickness of 20 and 70 nm, respectively.

For layered GO membranes,[2] water molecules permeate through the interlayer nanochannels formed between GO nanosheets and follow the 2D path over the hydrophobic non-oxidized surface rather than the hydrophilic oxidized region of GO. The interlayer spacing of the GO membranes increases to ~ 0.9 nm due to the hydration. It should be noted that the hydrophilic oxidized regions strongly interact with intercalating water and may not contribute for the water permeation. Larger ions and molecules than the interlayer spacing are blocked. For NS membranes, the clearance gap between sheets was only 0.2 nm for NS membranes and the interlayer spacing didn't increase in water so much because TEOA act as a chemical binder between sheets, implying that water cannot enter the interlayer between niobate sheets. Thus a model of nanochannels in the stacked NS membranes is suggested as shown in **Figure 2**(c). When the sheets are stacked, void structure forms as water pass through the thin membranes, resulting in the formation of nanochannels. The channels with nanosheet thickness-dependent size are created naturally during the vacuum filtration. The schematic diagram simply shows void structures formed by stacking with a piece of nanosheets in NS membranes (**Figure 2**(c), right). After all, given the results of Stokes-Einstein radius estimated from MWCO, void structures which are formed by stacking with several pieces of nanosheets became nanochannels in NS membranes. The possibility of size exclusion by pores which can be formed between sheets in lateral direction is relatively low because of the fact that rejection ratio doesn't increase with increase of the nanosheet thickness.

Rejection performances of the NS membranes with a thickness of 20 nm were studied using organic dyes (**Figure 3**(a)). The rejection of Evans Blue (EB, Mw: 960.8) was maintained at nearly 100% and that of Acid red 265 (Mw: 635.6) was 91.7 %. Thus high rejection performances of the organic dyes were achieved. Salts rejection is another important targets for NS membranes. The rejection for Na_2SO_4 and NaCl were 78.4 and 24.4 %, respectively. The surface charge of the NS membranes by ζ-potential was measured by streaming potential measurements and the rejection of NaCl was also investigated (**Figure 3**(b)). It was found that ζ-potential depends on pH and the iso-electric point (IEP) is about 6.7. The NS membranes was negatively charged in higher pH range. The rejection ratio of NaCl increases when the surface charge becomes negative. The negatively charged NS membranes resulted in a higher rejection to multivalent anion than monovalent anion, which followed the Donnan exclusion.[2829] **Table S1** summarizes the membrane performances of recent GO nanosheets NF membranes. It was found that the NS membranes exhibited superior flux and rejection ratio of salts as compared with GO membranes prepared by a similar vacuum filtration[611] and comparable performances to GO membranes prepared by an electric field assisted layer-by-layer assembly.[10] We attribute the high flux of NS membrane to the short water pathway because of the following two factors. First, relatively small lateral size of around 50 – 200 nm for the niobate nanosheets (**Figures 1**(a) and (b), ESI) enables the NS membranes to have a high aperture ratio on the top surface of membranes and the easy formation of void structures in the membranes. Secondly, the transport model suggested as shown in **Figure 2**(c) can directly explain the possible short water pathway as compared with the general water transport through the interlayer of GO nanosheets (ESI). These are reasons for the NS membranes bringing a significant benefit to the water flux.

Conclusions

In summary, we have demonstrated that niobate nanosheet nanofiltration membranes can be effectively prepared by a simple vacuum filtration on a modified nitrocellulose support using colloidal solution of 2D molecular sheet. The nanosheet membranes has a dense and stable structure in water and exhibits short pathways for water molecules in the densely stacked nanosheets. As a result, the novel nanosheet NF membranes are demonstrated to show higher flux and rejection of salts as compared with reported graphene oxide NF membranes, which are important performances for desalination or water purification in future. The preparation of such 2D nanosheet membranes is also expected to be expandable to prepare other transition metal oxide nanosheet membranes, which may open up valuable perspectives for wider applications in functional membranes.

Notes and references

1 C. C. Striemer, T. R. Gaborski, J. L. McGrath and P. M. Fauchet, *Nature*, 2007, **445**, 749–753.

2 R. R. Nair, H. A. Wu, P. N. Jayaram, I. V. Grigorieva and A. K. Geim, *Science (80-.).*, 2012, **335**, 442–444.

3 H. Huang, Z. Song, N. Wei, L. Shi, Y. Mao, Y. Ying, L. Sun, Z. Xu and X. Peng, *Nat. Commun.*, 2013, **4**, 2979–2987.

4 H. Huang, Y. Mao, Y. Ying, Y. Liu, L. Sun and X. Peng, *Chem. Commun.*, 2013, **49**, 5963–5965.

5 M. Hu and B. Mi, *Environ. Sci. Technol.*, 2013, **47**, 3715–3723.

6 Y. Han, Z. Xu and C. Gao, *Adv. Funct. Mater.*, 2013, **23**, 3693–3700.

7 K. Huang, G. Liu, Y. Lou, Z. Dong, J. Shen and W. Jin, *Angew. Chemie - Int. Ed.*, 2014, **53**, 6929–6932.

8 R. K. Joshi, P. Carbone, F. C. Wang, V. G. Kravets, Y. Su, I. V Grigorieva, H. A. Wu, A. K. Geim and R. R. Nair, *Science*, 2014, **343**, 752–4.

9 H. Huang, Y. Ying and X. Peng, *J. Mater. Chem. A*, 2014, **2**, 13772–13782.

10 T. Wang, J. Lu, L. Mao and Z. Wang, *J. Memb. Sci.*, 2016, **515**, 125–133.

11 J. Wang, P. Zhang, B. Liang, Y. Liu, T. Xu, L. Wang, B. Cao and K. Pan, *ACS Appl. Mater. Interfaces*, 2016, **8**, 6211–6218.

12 L. Sun, H. Huang and X. Peng, *Chem. Commun. (Camb).*, 2013, **49**, 10718–20.

13 L. Sun, Y. Ying, H. Huang, Z. Song, Y. Mao, Z. Xu and X. Peng, *ACS Nano*, 2014, **8**, 6304–6311.

14 R. Schaak and T. E. Mallouk, *Chem. Mater.*, 2000, **12**, 2513–2516.

15 T. Sasaki, S. Nakano, S. Yamauchi and M. Watanabe, *Chem. Mater.*, 1997, **9**, 602–608.

16 A. Takagaki, M. Sugisawa, D. Lu, J. N. Kondo, M. Hara, K. Domen and S. Hayashi, *J. Am. Chem. Soc.*, 2003, **125**, 5479–5485.

17 Y. Ebina, T. Sasaki, M. Harada and M. Watanabe, *Chem. Mater.*, 2002, **14**, 4390–4395.

18 Y. Okamoto, S. Ida, J. Hyodo, H. Hagiwara and T. Ishihara, *J. Am. Chem. Soc.*, 2011, **133**, 18034–1803.

19 E. Sabio, R. Chamousis, N. D. Browning and F. E. Osterloh, *J. Phys. Chem. C*, 2012, **116**, 3161−3170.

20 K. Nakagawa, T. Jia, W. Zheng, S. M. Fairclough, M. Katoh, S. Sugiyama and S. C. E. Tsang, *Chem. Commun.*, 2014, **50**, 13702–13705.

21 P. Sun, Q. Chen, X. Li, H. Liu, K. Wang, M. Zhong, J. Wei, D. Wu, R. Ma, T. Sasaki and H. Zhu, *NPG Asia Mater.*, 2015, **7**, e162.

22 P. Sun, R. Ma, W. Ma, J. Wu, K. Wang, T. Sasaki and H. Zhu, *NPG Asia Mater.*, 2016, **8**, e259.

23 C.-N. Yeh, K. Raidongia, J. Shao, Q.-H. Yang and J. Huang, *Nat. Chem.*, 2015, **7**, 166–170.

24 D. C. Marcano, D. V. Kosynkin, J. M. Berlin, A. Sinitskii, Z. Sun, A. Slesarev, L. B. Alemany, W. Lu and J. M. Tour, *ACS Nano*, 2010, **4**, 4806–4814.

25 L. Bartouilh de Taillac, M. C. Porté-Durrieu, C. Labrugère, R. Bareille, J. Amédée and C. Baquey, *Compos. Sci. Technol.*, 2004, **64**, 827–837.

26 A. Huang, W. Dou and J. Caro, *J. Am. Chem. Soc.*, 2010, **132**, 15562–15564.
27 C. M. Tam and A. Y. Tremblay, *J. Memb. Sci.*, 1991, **57**, 271–287.
28 T. Tsuru, D. Hironaka, T. Yoshioka and M. Asaeda, *Sep. Purif. Technol.*, 2001, **25**, 307–314.
29 N. Hilal, H. Al-Zoubi, N. A. Darwish, A. W. Mohamma and M. Abu Arabi, *Desalination*, 2004, **170**, 281–308.